PRAMANA
— journal of
physics

Vol. 66, No. 1
January 2006
pp. 3–30

Vortices in Bose–Einstein condensates: A review of the experimental results

R SRINIVASAN
Raman Research Institute, C.V. Raman Avenue, Sadashivanagar, Bangalore 560 080, India
E-mail: rsv@rri.res.in

Abstract. Rotating dilute Bose–Einstein condensates (BEC) of alkali atoms offer a testing ground for theories of vortices in weakly interacting superfluids. In a rotating superfluid, quantised vortices, with a vorticity h/m, form above a critical velocity. Such vortices have been generated in BEC of alkali atoms by different techniques such as (a) wave function engineering of a two-component BEC, (b) decay of solitons, (c) rotation of a thermal cloud before cooling it below the condensation temperature, (d) stirring with an 'optical' spoon, (e) rotating a deformation in the anisotropic trap in which the condensate is trapped and (f) by creating Berry phase by adiabatically reversing the axial magnetic field. Since the core of a vortex is a fraction of a micrometer in diameter, it cannot be directly imaged optically. The condensate with vortices is allowed to ballistically expand till the size increases by one order before the vortices are imaged. Surface wave spectroscopy and the change in aspect ratio of a rotating cloud are the other techniques used.

Studies have been made on the creation and dynamics of single vortex and on systems with more than a hundred vortices. Results have been obtained on vortex nucleation, stability of vortex structures, nature of the vortex lattice and defects in such a lattice. Important results are: (a) evidence exists that vortex nucleation takes place by a surface mode instability; but this is not the only mechanism; (b) the vortex lattice is perfectly triangular right up to the edge; (c) in the initial stages of rotation of the cloud a tangled web of vortices is seen; it takes a few hundred milliseconds before the vortices arrange themselves in a lattice; this time appears to be independent of temperature; (d) the decay of vortices appears to arise from the transfer of energy to the rotating thermal component and is dependent on temperature; (e) defects in the lattices such as dislocations and grain boundaries are seen; (f) transverse oscillations (Tkachenko modes) of the vortex lattice have been observed; and (g) giant vortices have been produced. These will be discussed.

Keywords. Bose–Einstein condensate; vortices; Gross–Pitaevski equation.

PACS Nos 03.75.Kk; 03.80.Pg; 67.40.Db

1. Introduction

Atoms such as ^{4}He, ^{7}Li, ^{23}Na and ^{87}Rb have total nuclear and electronic spin quantum number, which is zero or an integer. Such atoms obey Bose–Einstein statistics. In this statistics there is no restriction on the number of particles occupying any quantum state. One consequence of this statistics is the condensation of a macroscopic fraction of the particles in the ground state when the particles are cooled

below a temperature T_c, called the condensation temperature. If the atoms are trapped in a harmonic potential, the condensation temperature is proportional to the 1/3 power of the total number of atoms in the trap.

Liquid ^{4}He under atmospheric pressure shows a phase transition below 2.17 K. The liquid below this temperature is called liquid HeII and exhibits unusual physical properties, which have been studied thoroughly over several decades. It was London who suggested that this phase transition is a Bose–Einstein condensation. At the density of liquid helium the interaction between the atoms is strong. There is no many-body theory for strongly interacting Bose particles with which the experimental results could be compared. The theory of weakly interacting bosons, however, has been worked out in detail.

The alkali atoms ^{7}Li, ^{23}Na and ^{87}Rb can exist in a long-lived metastable vapour state of low density even when they are cooled to a few tens of nano-kelvin. At a pressure of 10^{-11} mbar, a cloud of such atoms can be initially laser cooled to a few tens of a micro-Kelvin and trapped in a magnetic trap. They can be further cooled by RF-assisted evaporative cooling to a temperature below T_c at the density obtaining in the trap. Thus one can realise Bose–Einstein condensation in a cloud of alkali atoms. The density of atoms in the condensate is of the order of 10^{14} atoms/cc and the transition temperature is of the order of 100 nano-Kelvin. Bose–Einstein condensation has been achieved in ^{87}Rb [1], ^{23}Na [2] and ^{7}Li [3]. It has been possible to obtain about 10^6 to 10^7 atoms in the condensate in the first two cases. The temperature can be lowered to a few tens of a nano-Kelvin so that the fraction of atoms in the excited state is negligible. In Ioffe–Pritchard magnetic traps in which the BEC is obtained, the trap frequency along the z-axis is much lower than the trap frequency in the xy plane. So the cloud is cigar-shaped with a high aspect ratio. One can also use a TOP trap. In this case the axial trap frequency is more than the radial trap frequency. The condensate is disc shaped. Many properties of BEC in such traps have been studied.

The following aspects are noteworthy. At the densities obtainable in these clouds the interaction between the atoms is weak and it is predominantly described by the s wave scattering length, a. The scattering length is of the order of a few nanometers while the distance between the atoms is 100 times larger. A positive scattering length, a, indicates a repulsive interaction. In such a case there is no limit to the number of atoms in the condensate and one can obtain stable condensates with a million atoms or more. This is the situation with ^{87}Rb and ^{23}Na. If the scattering length is negative, the interaction between the atoms is attractive. In this case there is a limit to the number of atoms in the condensate. When this limit is exceeded there is a collapse of the condensate. This is the case with ^{7}Li.

The BEC in alkali atoms provide a convenient testing ground for many-body theory of weakly interacting Bose particles.

Before discussing the experimental results on vortices in BEC of alkali atoms, we shall highlight the salient points of theory relevant to our discussion.

2. Ground state of a BEC: The Gross–Pitaevski equation

Dalfovo *et al* [4] have reviewed the theory of the trapped condensate. The condensate can be described by a complex order parameter in the spirit of Landau's theory

of phase transition. This order parameter ϕ has a magnitude and a phase. The magnitude is the square root of the number density of atoms in the condensate. We may therefore write

$$\phi(\mathbf{r},t) = \sqrt{n(\mathbf{r},t)}\exp(i)S(\mathbf{r},t). \tag{2.1}$$

In the mean-field approximation the order parameter will satisfy the Gross–Pitaevski equation

$$i\hbar\partial\phi(\mathbf{r},t)/\partial t = \left[(-\hbar^2/2m)\nabla^2 + V_{\text{ext}}(\mathbf{r}) + g|\phi(\mathbf{r},t)|^2\right]\phi(\mathbf{r},t). \tag{2.2}$$

Here m is the mass of the atom, $V_{\text{ext}}(\mathbf{r})$ is the harmonic trap potential and

$$g = 4\pi\hbar^2 a/m \tag{2.3}$$

is the interaction energy between the atoms expressed in terms of the scattering length a.

If we are working in the steady state, the left side of the equation is replaced by $\mu\phi(\mathbf{r})$ so that eq. (2.2) becomes

$$\left[(-\hbar^2/2m)\nabla^2 + V_{\text{ext}}(\mathbf{r}) + g|\phi(\mathbf{r})|^2\right]\phi(\mathbf{r}) = \mu\phi(\mathbf{r}). \tag{2.4}$$

Here μ is the chemical potential. The interaction is considered to be weak if $na^3 \ll 1$, where n is the number density of atoms. The maximum number density in the condensates achieved so far is 10^{15}/cc. a is of the order of nanometers. So the above condition is well satisfied in these condensates.

Since the temperatures are in the nano-Kelvin region the kinetic energy of the particles is low. At the number densities in the condensate the interaction energy term, gn, can be much larger than the kinetic energy. In such a case we can neglect the first term involving ∇^2 in eq. (2.4) and write

$$|\phi(\mathbf{r})|^2 = [\mu - V_{\text{ext}}(\mathbf{r})]/g. \tag{2.5}$$

This is called the Thomas–Fermi approximation. For a harmonic trap

$$V_{\text{ext}}(\mathbf{r}) = (1/2)m[\omega_x^2 x^2 + \omega_y^2 y^2 + \omega_z^2 z^2], \tag{2.6}$$

where $\omega_j = 2\pi\nu_j$ and ν_x, ν_y and ν_z are the trap frequencies along the principal axes of the trap. One defines a geometric mean frequency

$$\bar{\omega} = (\omega_x\omega_y\omega_z)^{1/3} \tag{2.7}$$

and an arithmetic mean frequency

$$\omega_{\text{av}} = (\omega_x + \omega_y + \omega_z)/3. \tag{2.8}$$

From eqs (2.5) and (2.6) we see that the density along the x or y or z axis will have a maximum value at the origin and will decrease parabolically to zero as one moves away from the origin. In a trap the density is inhomogeneous.

Substituting in eq. (2.4) for $\phi(\mathbf{r},t)$, from eq. (2.1), the following equations can be obtained for $n(\mathbf{r},t)$ and $S(\mathbf{r},t)$.

$$\partial n/\partial t + \nabla \cdot [n(\hbar/m)\text{grad } S] = 0, \tag{2.9}$$

$$\hbar\,\partial S/\partial t + (1/2m)(\hbar\,\text{grad } S)^2 + V_{\text{ext}} + gn - (\hbar^2/2m)(1/\sqrt{n})\nabla^2(\sqrt{n}) = 0. \tag{2.10}$$

The current density

$$j = i(\hbar/2m)(\phi\nabla\phi^* - \phi^*\nabla\phi). \tag{2.11}$$

Substituting for ϕ from eq. (2.1)

$$j = n(\hbar/m)\nabla S. \tag{2.12}$$

The velocity v of the condensate may now be identified as

$$\mathbf{v} = (\hbar/m)\nabla S. \tag{2.13}$$

So

$$\text{Curl } \mathbf{v} = 0. \tag{2.14}$$

In a singly-connected region in the condensate

$$\oint_c \mathbf{v} \cdot \mathrm{d}\mathbf{r} = 0. \tag{2.15}$$

The flow of the fluid is irrotational. The condensate is a superfluid.

If we substitute for the velocity $\mathbf{v}$ in terms of eq. (2.13), we see that eqs (2.9) and (2.10) are equivalent to the equation of continuity and the classical equation of conservation of energy of an inviscid fluid except for the term $-(\hbar^2/2m)(1/\sqrt{n})\nabla^2(\sqrt{n})$. This term gives rise to the quantum pressure in the equation of motion. Its magnitude becomes negligible compared to the other terms in eq. (2.10), if the number of atoms in the trap tends to infinity. However for the number of atoms realised in the BEC of alkali atoms it does make a significant contribution, for example to the surface mode frequencies.

3. Collective excitations of the condensate

Writing

$$\phi(\mathbf{r}, t) = \exp(-i\mu t/\hbar)\,\{\phi(\mathbf{r}) + u(\mathbf{r})\exp -i\omega t + v^*(\mathbf{r})\exp i\omega t\} \tag{3.1}$$

in the time-dependent Gross–Pitaevski equation (2.2) and keeping terms linear in u and v we get two coupled equations

$$\hbar\omega u(\mathbf{r}) = \left\{H_0 - \mu + 2g|\phi(\mathbf{r})|^2\right\} u(\mathbf{r}) + g|\phi(\mathbf{r})|^2 v(\mathbf{r}) \tag{3.2a}$$

and

$$-\hbar\omega v(\mathbf{r}) = \left\{H_0 - \mu + 2g|\phi(\mathbf{r})|^2\right\} v(\mathbf{r}) + g|\phi(\mathbf{r})|^2 u(\mathbf{r}). \tag{3.2b}$$

Here

$$H_0 = (\hbar^2/2m)\nabla^2 + V_{\text{ext}}(\mathbf{r}). \tag{3.3}$$

The eigenfrequencies of the coupled equations give the collective excitation frequencies. At low frequencies of the order of $\bar{\omega}$, the collective excitations correspond to deformational motion of the trapped cloud. For a harmonic spherical trap ($\omega_x = \omega_y = \omega_z$) these deformations in density can be written in the form

$$\delta n(\mathbf{r}) = P_\ell^{(2n)}(r/R) r^\ell Y_{\ell m}(\theta, \phi), \tag{3.4}$$

where $P^{(2n)}(r/R)$ are polynomials of degree $2n$ containing only even powers of the argument (r/R) and $Y_{\ell m}(\theta, \phi)$ are the spherical harmonics. R is the radius of the cloud. n is the number of radial nodes. The dispersion law of the discrete normal modes, in the limit the quantum pressure term is negligible, and is given by

$$\omega(n, \ell) = \bar{\omega}[2n^2 + 2n\ell + 3n + \ell]^{1/2}. \tag{3.5}$$

The surface modes correspond to $n = 0$ and the compressional modes to $n \neq 0$. For a given n and ℓ the frequency is independent of m.

For an axially symmetric trap

$$\omega_x = \omega_y = \omega_\perp \neq \omega_z. \tag{3.6}$$

In this case the dispersion law depends on m. For the surface mode $\ell = 2$ and $m = \pm 2$ explicit results can be obtained in the hydrodynamic limit, namely

$$\omega^2(\ell = 2, m = \pm 2) = 2\omega_\perp^2. \tag{3.7}$$

We note that the frequency of this mode is the same for $m = 2$ and $m = -2$. In the mode $m = 2$, the cross-section of the cloud in the xy plane is elliptical and the ellipse rotates counterclockwise with the frequency ω. For the mode $m = -2$ the cross-section rotates in the clockwise direction with the same frequency. *In the presence of vortices, these two frequencies are different.* This has been used to detect the generation of vortices and to measure their number.

4. A rotating condensate: Creation of a vortex state

In a rotating condensate a vortex can be formed. In the presence of the vortex along the z-axis, the order parameter varies as

$$\phi(\mathbf{r}) = \phi_v(\rho, z) \exp i\kappa\phi. \tag{4.1}$$

The suffix v on ϕ is to show that this is a vortex state. Here ρ, ϕ, z are the cylindrical coordinates of a point and κ is an integer. Note that the phase ϕ varies in a closed path from 0 to 2π. One way of creating a vortex is to imprint such a phase in the condensate.

The velocity of the fluid is given by

$$\mathbf{v} = (\hbar/m\rho)\kappa\mathbf{e}_\phi, \tag{4.2}$$

where $\mathbf{e}_\phi$ is a unit vector in the tangential direction in the xy plane. The circulation integral around the z-axis is

$$\oint \mathbf{v} \cdot \mathrm{d}\mathbf{r} = \kappa h/m \tag{4.3}$$

and the angular momentum of the condensate around the z-axis is

$$L_z = N\kappa\hbar. \tag{4.4}$$

The presence of the angular momentum introduces an additional centrifugal potential in the Gross–Pitaevski equation. The equation now becomes

$$\left[(-\hbar^2/2m)\nabla^2 + (\hbar^2\kappa^2/2m\rho^2) + V_{\mathrm{ext}}(\mathbf{r}) + g|\phi(\mathbf{r})|^2\right]\phi(\mathbf{r}) = \mu\phi(\mathbf{r}) \tag{4.5}$$

with the corresponding axially symmetric trap potential $V_{\mathrm{ext}}(\mathbf{r})$.

Because of the centrifugal potential the solution must be one in which $\phi_v(\mathbf{r})$ goes to zero as ρ tends to zero. The density of the fluid increases from zero along the axis of the vortex and reaches a maximum value at a distance ρ_m. In the absence of the vortex the density is a maximum along the axis. The region in which the density is depleted is called the core of the vortex. At $T = 0$, when only the condensate is present, the core is empty of atoms. But at a finite temperature, the core can be filled by atoms in the excited states. One can define a quantity, ξ, called the healing length by the equation

$$\xi = (8\pi na)^{-1/2}. \tag{4.6}$$

In a condensate in a trap, the density n is not a constant. Taking the maximum density n_{max}, the value of ξ is of the order of a fraction of a micrometer. The diameter of the vortex core in the condensate is of the same order as ξ. Compare it with the diameter of the vortex core in superfluid helium, which is of the order of an Angstrom.

Since the alkali condensates are either imaged in absorption or in phase contrast using light resonant with the absorption frequency, a direct *in situ* imaging of the vortex core is not possible. When the trap is switched off, the atoms expand ballistically through mutual repulsion. In a few milliseconds the expansion will increase the core size by one order of magnitude. Now optical imaging will reveal the vortex core.

As the condensate is set in rotation, a vortex first appears with $\kappa = 1$ when the angular velocity Ω exceeds a critical value $\Omega_{\mathrm{c,th}}$. In the frame rotating with an angular velocity Ω, one will have to add to the Hamiltonian an additional term $-\Omega L_z$. The energy of the system with the angular momentum L_z in the rotating frame is $(E - \Omega L_z)$. E is the energy in the laboratory frame. For low rotational velocities Ω, the energy is minimal without the vortex (i.e. $L_z = 0$). But as Ω increases, the term $-\Omega L_z$ will increase in importance. Beyond a thermodynamic critical angular velocity $\Omega_{\mathrm{c,th}}$, the minimum energy is achieved in the presence of

a vortex with $\kappa = 1$. Calculations indicate that this critical angular frequency is of the order of (but smaller than) the trap frequency $\Omega_\perp$. The critical angular frequency decreases as the number of atoms in the trap increases. Lundh *et al* [5] found the following analytical expression for the critical angular frequency $\Omega_{\mathrm{c,th}}$.

$$\Omega_{\mathrm{c,th}} = (5\hbar/2mR_\perp^2)\ln(0.671R_\perp/\xi) \tag{4.7}$$

in the limit of large number of particles in the trap. $R_\perp$ is the radial extent of the cloud in the $z = 0$ plane.

As the angular velocity increases, one can create vortex states with κ values 2, 3, ... However if interaction between vortices is taken into account, a single vortex with vorticity κ has a higher energy than κ vortices with unit vorticity. So at high rotation frequencies, we should see many vortices each with unit vorticity.

We now have the requisite theoretical background to review the experiments.

5. Methods for creation of a vortex in the condensate

The following methods have been used to create vortices in the condensate.

5.1 *By phase imprinting in the condensate*

Phase imprinting can be done by either of the two methods. In the first method, in which phase imprinting is done dynamically, the phase of the condensate evolves according to the time integral of its energy and this can be tailored locally by a spatially varying external potential. Williams and Holland [6] suggested using a two-component condensate trapped in overlapping potentials. While the traps are rotated around each other at a frequency ω, one can transfer coherently atoms from a state $|1\rangle$ to a state $|2\rangle$ at a Rabi frequency Ω by using electromagnetic radiation detuned by δ. The rotational frequency compensates for the detuning.

This scheme was implemented by Mathews *et al* [7] in a two-component condensate of ^{87}Rb. The two hyperfine ground states $F = 1$ and $F = 2$ of the atom form the two component condensate in overlapping magnetic traps. About 8×10^5 atoms in state $|1\rangle$ are trapped in a time orbiting potential (TOP) trap. The condensate is then transferred adiabatically to a spherical trap by reducing the quadrupole magnetic field. The atoms in this condensate have a lifetime of 75 s. A suitable oscillating magnetic field at a microwave frequency is applied to the condensate to cause a two-photon transition to state $|2\rangle$. To imprint a phase in the condensate in state $|2\rangle$, a 10 nW, 780 nm laser beam, detuned by 0.8 GHz to the blue of the resonant excitation from state $|2\rangle$, is focussed at the edge of the condensate to produce an AC Stark shift of the level $|2\rangle$ (see figure 1). This beam is rotated with piezoelectric actuators in a circle of 75 μm radius at a frequency ω which compensates for the detuning δ (if it is large) of the two-photon microwave field and causes a resonant transfer of atoms from state $|1\rangle$ to state $|2\rangle$. By adjusting the detuning, nearly 50% of the atoms can be resonantly transferred from state $|1\rangle$ to state $|2\rangle$. The atoms in state $|2\rangle$ then form a condensate with a phase winding

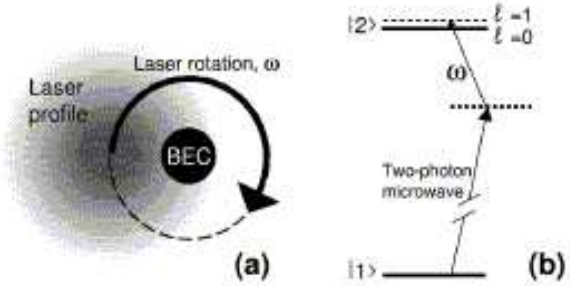

Figure 1. Schematic representation of phase imprinting technique in a two-component condensate [7].

of 2π imprinted on the condensate. This generates a vortex state in condensate in state $|2\rangle$.

On the other hand, if the laser beam is toggled from left to right at a frequency ω one can create a dark soliton. We have a band separating two regions in which coherently excited atoms exist in $|2\rangle$. However the phase of the condensate $|2\rangle$ on one side of the band is π relative to the phase of the condensate on the other side. The density of atoms in $|2\rangle$ in the dividing band is zero. This is called a dark soliton. The dark soliton will break up into two vortex rings. This has been demonstrated by Anderson *et al* [8].

The vortex core or the soliton ridge can be filled with atoms in the condensate state $|1\rangle$ in which the vortex state or soliton state is absent. The repulsion of the atoms in the core enlarges the core and contributes to the stability of the vortex.

One can also imprint a phase on a condensate topologically [9]. Let us consider atoms in the condensate in an Ioffe–Pritchard trap. In this trap the magnetic field **B** is given by

$$\mathbf{B} = B_z \mathbf{e}_z + B'(x\mathbf{e}_x - y\mathbf{e}_y) \tag{5.1}$$

with the condition

$$B_z \gg B'R > 0. \tag{5.2}$$

B' is the quadrupolar field gradient in the xy plane and R is the radius of the cloud in the xy plane. Consider two atoms in the xy plane at azimuthal angles ϕ_1 and ϕ_2. The two-dimensional quadrupolar field is pointing in the directions $\mathbf{b}_{\phi 1}$ at ϕ_1 and $\mathbf{b}_{\phi 2}$ at ϕ_2. As the direction of the z component B_z is adiabatically reversed, the angular momentum vector rotates about the direction $\mathbf{n}_\phi$ at the azimuthal angle ϕ as shown in figure 2a. The vector **F** rotates on a circle of radius $|m_F|\hbar$ as shown in figure 2b. If we take an atom at a point 1 with azimuthal angle ϕ_1, the Berry phase acquired by the order parameter after traversing a closed contour C on the sphere is $\gamma(C)$ where

$$\gamma(C) = -m_{\mathrm{F}}\Omega(C). \tag{5.3}$$

$\Omega(C)$ is the solid angle subtended by the contour at the centre of the sphere. If we close the contour via the path passing through ϕ_2, we get the topological phase

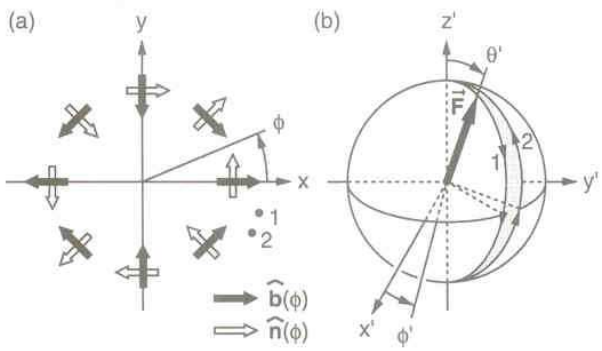

Figure 2. Figure (**a**) indicates the direction of the quadrupolar field $\mathbf{b}(\phi)$ at an azimuthal angle ϕ in the xy plane in an Ioffe–Pritchard trap. As the z component of the magnetic field is reversed, the angular momentum vector $\mathbf{F}$ rotates about the direction of $\mathbf{n}(\phi)$ for a point in the xy plane with an azimuthal angle ϕ (from ref. [10]). Figure (**b**) illustrates how the Berry phase arises as the angular momentum traces a great arc passing through the point 1 on a sphere of radius $m_{\mathrm{F}}\hbar$.

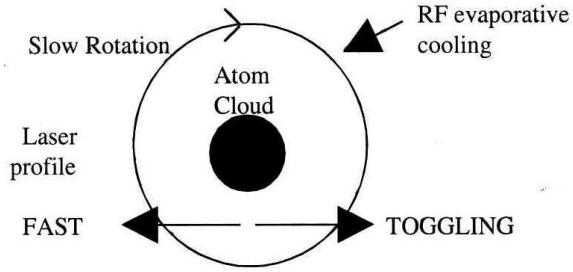

Figure 3. Rotation of the vapour of ^{87}Rb as it is cooled in an Ioffe–Pritchard trap. The plane shown is perpendicular to the axis of the Ioffe–Pritchard trap. Far-detuned laser beam travelling parallel to the axis and focussed 8 μm away from the axis is toggled at 100 kHz from right to left. At the same time the laser spot is rotated slowly at the rate Ω about the axis. The cloud is cooled by RF evaporative cooling to below T_{c}.

difference of the order parameter at the points 1 and 2 imprinted by reversing the field. Since the solid angle for the path shown in figure 2b is $2(\phi_1 - \phi_2)$ the phase difference is

$$\gamma(\phi_1) - \gamma(\phi_2) = -2m_{\mathrm{F}}(\phi_1 - \phi_2). \tag{5.4}$$

So the topological phase imprinted on the order parameter at an azimuthal angle ϕ is

$$\gamma(\phi) = -2m_{\mathrm{F}}\phi. \tag{5.5}$$

This corresponds to a vortex with $\kappa = 2m_{\mathrm{F}}$.

This was implemented by Leanhardt *et al* [10]. A condensate containing 10^7 ^{23}Na atoms in the $|1,-1\rangle$ state was transferred by an optical tweezer into the science chamber. There the atoms were converted to the $|2,2\rangle$ state and trapped in a micro fabricated Ioffe–Pritchard trap formed by a Z-shaped wire carrying a current with an external magnetic field $B_\perp$. The values of the field components were $B_z = 1$ G, $B_\perp = 5.4$ G and the radial field gradient $B' = 120$ G/cm. B_z was reversed. Vortices created by reversing B_z were observed after ballistic expansion. These should be multiply-charged vortices.

5.2 *By rotating a gas of bosonic atoms while cooling them to reach the condensation temperature* [11]

This technique is analogous to the rotating bucket experiment with liquid helium. Liquid helium I is in a bucket, which is rotated about a vertical axis at an angular frequency Ω. Because of the surface roughness of the bucket LHeI is set in rotation. It is cooled during rotation to below the transition temperature. If the rotation frequency is more than the critical frequency then a vortex state is created in LHeII.

In the experiment, ^{87}Rb atoms are confined in an Ioffe–Pritchard trap above the condensation temperature. RF evaporation is started with an initial frequency of 15 MHz. This frequency is exponentially decreased to a final value ν^{final} in 25 s with a time constant of 5.9 s. When ν^{final} is 480 kHz condensation starts and the condensation temperature is 500 nK. 430 kHz is the value of the RF frequency to empty the trap completely. When the evaporating radio frequency reaches a value of 510 kHz a stirring laser beam (of wavelength 852 nm) travelling parallel to the slow axis of the trap is switched on. The beam power is 0.4 mW and the beam is focussed to a waist of 20 μm. The laser beam is far-detuned. Two motions, one fast and one slow are superimposed on the beam. The fast motion at 100 kHz (fast compared to the trap frequencies) toggles the beam axis between two positions symmetrically situated about the axis of the trap and 8 μm away from the axis. At the same time the beam axis is slowly rotated about the axis of the trap at an angular frequency Ω, which is kept constant at a value between 0 and 250 radian/s. This is schematically illustrated in figure 3.

In the absence of the laser beam the trap potential is axially symmetric. Fast toggling of the laser beam creates two dimples in the time-averaged potential symmetrically about the trap axis. This produces the surface roughness of the trap, which sets the cloud into rotation at the frequency Ω. By increasing Ω one could verify at what critical frequency a vortex appears. As the frequency is increased further one can also verify whether single vortices with $\kappa = 2, 3, \ldots$ appear or whether κ singly quantised vortices appear. This method has also been followed by the Oxford group [12].

Haljan *et al* [13] performed experiments on ^{87}Rb atoms slightly above T_c in a TOP trap. In the TOP trap the cloud is disc-shaped because the axial frequency of the trap is more than the radial frequency. A very large ellipticity (about 25%) of the trap potential is induced in the XY plane and this anisotropy is rotated with a rate up to 2.5 Hz. Such a large ellipticity is required to rotate the normal cloud and to sustain its rotation. The normal cloud of atoms rotates with this angular velocity.

RF evaporative cooling is now applied selectively to remove atoms along the axis. For this purpose the oblate trap is adiabatically distorted into a prolate trap so that the extension of the cloud is larger along the axis and evaporative cooling preferentially removes the atoms along the axis. This is done so that the angular momentum of the cloud remains constant as the evaporative cooling proceeds.

Due to rotation, the aspect ratio of the cloud defined as $\lambda = \sigma_z/\sigma_\rho$ (σ_j is the extension of the cloud in the jth direction) changes. This change in aspect ratio arises because of the centrifugal potential due to rotation. The trap frequency $\omega_\perp$ is altered by rotation to $(\omega_\perp^2 - \Omega^2)^{1/2}$. One can relate the angular frequency of rotation to the aspect ratio by the equation

$$\Omega/\omega_\perp = [1 - (\lambda/\lambda_0)]^{1/2}, \tag{5.6}$$

where $\omega_\perp$ is the radial trap frequency and λ_0 is the aspect ratio in the TOP trap without rotation. As the cooling proceeds the aspect ratio λ decreases indicating that the rotational speed increases. When the condensate is rotating the speed of rotation is measured by measuring its aspect ratio. The presence of vortices is confirmed by looking at the difference in the surface mode frequencies $\ell = 2$ ($m = +2$) and $\ell = 2$ ($m = -2$). It was estimated that up to 56 vortices are formed in the condensate by this process.

5.3 *Stirring a trap containing the condensate with an optical spoon* [14]

The MIT group started with a condensate in a trap, which was stirred. A nearly pure condensate of 5×10^7 atoms of ^{23}Na, with no thermal component, was produced in a trap with weak asymmetry ($\nu_z = 20$ Hz and $\nu_\perp = 84$ Hz). The Thomas–Fermi radius of the condensate perpendicular to the z-axis was 29 μm. This was stirred by the optical dipole force exerted by a blue detuned (532 nm) laser beam. Using acousto-optic deflectors two laser beams were derived at this wavelength and rotated at an angular frequency Ω around the z-axis. The laser beams were separated by 25 μm, which was also the size of the waist of the Gaussian beams. The laser power was 0.7 mW. After producing the condensate the power of the rotating beams was ramped up in 20 ms, held constant for a variable spinning time and then ramped down in 20 ms. The condensate was allowed to equilibrate for 500 ms in the trap. The trap was then switched off and the condensate allowed to expand ballistically. Resonant absorption imaging revealed the presence of an ordered triangular lattice of vortices.

6. Detecting the presence of vortices

6.1 *Surface wave spectroscopy*

In the absence of spinning, the condensate has an aspect ratio, λ_0 in a plane containing the axis of rotation. If the condensate spins with an angular velocity Ω, the aspect ratio decreases to a value λ. The relation between the angular velocity Ω,

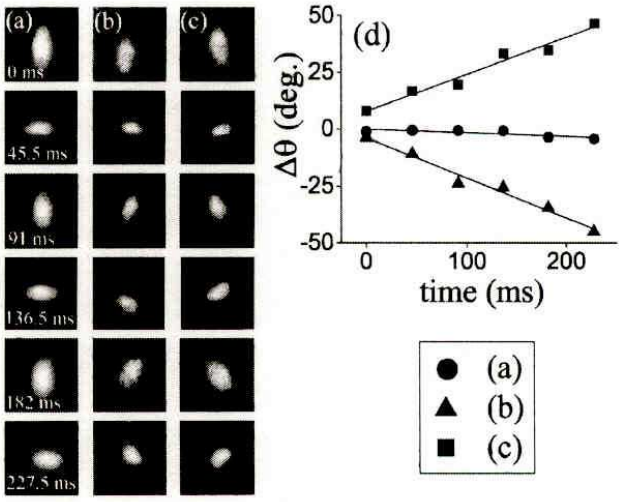

Figure 4. Quadrupolar modes excited in (**a**) a vortex free condensate of ^{87}Rb, (**b**) and (**c**) are quadrupolar modes in a condensate with a vortex. The images are non-destructive and strobed at intervals of 45.5 ms. The trap frequency $\nu_\perp = 7.8$ Hz [16]. The linear fit to the angle of rotation as a function yields a value − 0.49(4) Hz for the precession frequency in (b) and 0.45(5) Hz for the precession frequency in (c).

the trap frequency $\omega_\perp$, and the aspect ratio λ is given by eq. (5.6). The angular velocity of an oblate condensate was determined in this fashion by Haljan *et al* [13].

The quadrupolar surface modes $\ell = 2$, $m_\ell = \pm 2$ of an axially symmetric condensate have the same frequency $\omega = \sqrt{2}\omega_\perp$. However if the condensate has an angular momentum, then the degeneracy is lifted. For small rotation rates, the splitting in frequency between the modes is directly proportional to the mean angular momentum of the condensate (see ref. [13]). Zambelli and Stringari [15] used a sum rule to show that for large values of Ω, the difference in frequencies of the two modes is 2Ω while the sum of the squared frequencies of the two modes is independent of the speed of rotation. The axis of the vortex is along the axis of rotation. The quadrupolar surface modes in a plane perpendicular to the axis of rotation can be excited by rotating a weak deformity in the magnetic trap [16]. In the mode $m = 2$, the deformed cloud in the xy plane is elliptical. The principal axes of the ellipse rotate counterclockwise for $m = +2$ and clockwise for $m = -2$. Non-destructive images of the deformed cloud are taken at periodic intervals. Figure 4 shows the sequence of images for (a) a vortex-free condensate in which both the modes are degenerate in frequency and (b) and (c) for condensates with a vortex [16]. (b) shows the mode $m = +2$ and (c) the mode $m = -2$. Note that the rotation in (c) is opposite to that in (b).

Using such a technique in combination with the change in aspect ratio to measure Ω, Haljan *et al* [13] verified Zambelli and Stringari's predictions as shown in the following figure 5. This technique has also been used by Madison *et al* [17].

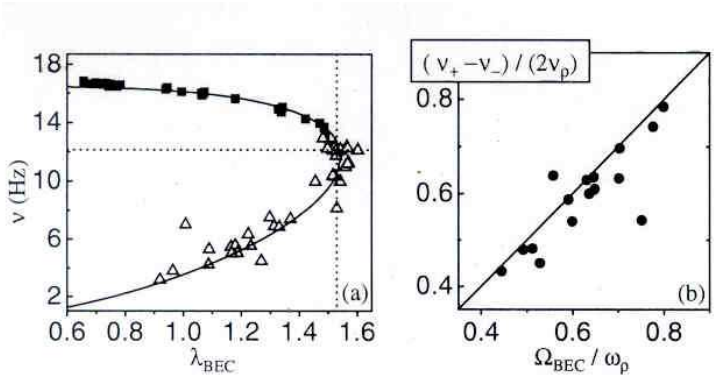

Figure 5. (**a**) Variation of the frequencies of the quadrupolar modes as a function of the aspect ratio. The continuous curve is the best fit from theory. (**b**) Frequency splitting of the quadrupolar modes as a function of $\Omega/\omega_\perp$ obtained from the aspect ratio λ using eq. (5.6).

6.2 *Direct observation of vortices*

It was mentioned earlier that the size of the vortex core is of the order of healing length ξ which is a fraction of a micrometer. Direct optical imaging of the bare core using resonant laser light is not possible. However in two component condensates the core of the vortex in one component can be filled by the atoms of the other component. The repulsion of these atoms may enlarge the size of the core to a point when *in situ* imaging with phase contrast technique is possible [18].

If we switch off the trap potential, the atoms expand ballistically. Dalfovo and Modugno [19] solved the time-dependent Gross–Pitaevski equation numerically to study the free expansion of a condensate containing vortices. The ratio of the core radius, ρ_c to the extension of the cloud, $R_\perp$, perpendicular to the axis of rotation in the condensate in a trap depends on, (a) the strength of the interaction energy and (b) the aspect ratio, λ_0. For cigar-shaped condensates, this ratio is larger than for disc-shaped condensates. The ratio decreases as the number of atoms in the trap increases. When the trap is switched off and the atoms are allowed to ballistically expand, the ratio increases with time and reaches a limiting value when the interaction energy decreases. This indicates that the core expands faster than the cloud reaching a size of the order of 10–50 μm. This rapid expansion of the core makes resonant imaging of the vortex cores possible after ballistic expansion.

This technique is most commonly used to image the vortex cores [11,14,20]. Absorption imaging is done about 50 ms after releasing the condensate.

7. Critical angular velocity for creation of vortices and vortex nucleation

It has already been mentioned in §3 that there is a thermodynamic critical angular velocity $\Omega_{c,th}$ above which a vortex state is created in the condensate. This is the

angular frequency at which the energy per particle $(E/N)_{\rm v}$ in the vortex state, measured in the laboratory frame, satisfies the condition

$$(E/N)_{\rm v} = (E/N)_{\rm g} + \Omega_{\rm c,th}\ell_z, \tag{7.1}$$

where $(E/N)_{\rm g}$ refers to the energy per particle in the vortex-free ground state of the condensate and $\ell_z = L_z/N$ is the angular momentum per particle.

Dalfovo *et al* [23] have made a numerical calculation of $\Omega_{\rm c,th}$ for three different traps with aspect ratios $\lambda = 0.0058$ (prolate), 1 (spherical) and 10 (oblate) with the same geometric mean frequency $\bar{\omega}$ (7.8 Hz) containing about 3×10^5 particles. They found the value of $\Omega_{\rm c,th}$ to be $0.35\omega_\perp$ for the prolate trap, $0.24\omega_\perp$ for the spherical trap and $0.12\omega_\perp$ for the oblate trap. These exactly calculated numerical values were within about 2% of the values calculated using eq. (3.6) of Lundh *et al* [5]. The first experiments of the ENS group [11,21,22] appeared to indicate that vortices first appeared in a condensate at much higher rotational velocities. In these experiments the rotation of the cloud was created by a focussed laser beam in a pattern to deform the trap potential quadrupolarly and create a surface mode. The observed critical angular frequencies were around $0.7\omega_\perp$.

That the critical angular frequency to form a vortex is higher than the thermodynamic critical value given by eq. (7.1) can be understood as follows. There is a surface barrier for the vortex to penetrate from the surface to the interior at the thermodynamic critical frequency. A vortex state can be formed only if this barrier becomes zero. This implies that the critical frequency $\Omega_{\rm c}$ should be the value of Ω at which one of the surface mode frequencies becomes zero in the rotating frame.

Dalfovo *et al* [23] used a sum rule to arrive at an upper bound for different surface excitation modes $\ell, m = \ell$. They obtained the dispersion relation

$$\omega_\ell^2 = \ell\omega_\perp^2 \left[1 + (\ell - 1)\beta_\ell\right], \tag{7.2}$$

where

$$\beta_\ell = \int {\rm d}\mathbf{r} (\nabla_\perp \sqrt{n})^2 \mathbf{r}_\perp^{2\ell-4} \Big/ \int {\rm d}\mathbf{r}\ n\mathbf{r}_\perp^{2\ell-2}, \tag{7.3}$$

n is the number density of atoms in the ground state and $\mathbf{r}_\perp^2 = x^2 + y^2$. For low values of ℓ, the frequencies calculated using the sum rule are very close in value to those calculated numerically. For large values of ℓ deviations are expected. However up to $\ell = 10$, the deviation from exact numerical calculations appear to be less than 10%. When Ω_ℓ equals the value of ω_ℓ the condensate becomes unstable to the excitation of this surface mode and energy is transferred to these surface excitations. One may derive a critical value for the rotation frequency $\Omega_{\rm c}$ as

$$\Omega_{\rm c} = \min\ (\omega_\ell/\ell). \tag{7.4}$$

As the number of atoms in the condensate tends to infinity, the hydrodynamic equations (neglecting the quantum pressure term) will be valid. The hydrodynamic equations give

$$\omega_\ell = \sqrt{\ell}\omega_\perp. \tag{7.5}$$

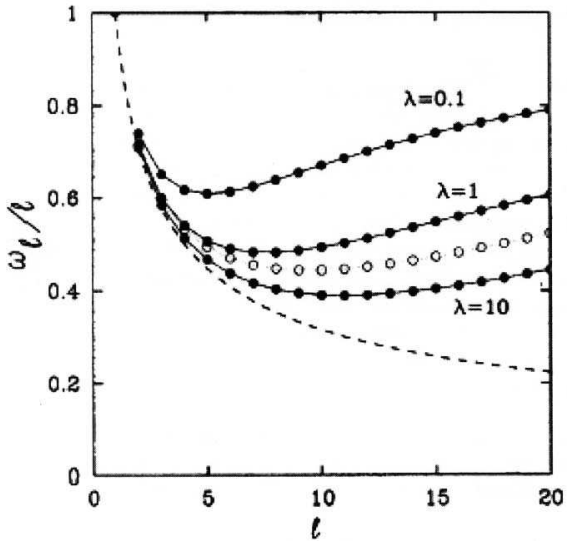

Figure 6. The quantity ω_ℓ/ℓ in units of $\omega_\perp$ as a function of ℓ for a condensate of ^{87}Rb for three trap aspect ratios $\lambda = \omega_z/\omega_\perp$. The total number of atoms $N = 10^5$ and the geometric mean frequency ω is 20 Hz. These results are obtained from the sum rule. Open circles represent exact solutions of Bogulibov's equation. Dashed line is the hydrodynamic prediction $\omega_\ell/\ell = 1/\sqrt{\ell}$.

Figure 6 shows the variation of ω_ℓ/ℓ as a function of ℓ in prolate ($\lambda < 1$), spherical ($\lambda = 1$) and oblate ($\lambda > 1$) traps for a total number N of 10^5 atoms with a geometric mean frequency $\bar{\nu}$ of 20 Hz as calculated by Dalfovo *et al* [23]. The dashed line indicates the dispersion in the hydrodynamic limit.

From eq. (7.5), it is obvious that in the hydrodynamic limit ($N \to \infty$) the critical angular velocity $\Omega_c = 0$. But with the number of atoms present in the trap around 10^5, quantum pressure term is sufficiently important to cause a deviation from the dispersion law in the hydrodynamic limit. The important findings of this paper are, (1) that for the quadrupolar mode $\ell = 2$, the value of $\omega_2/2$ is very close to the hydrodynamic value $1/\sqrt{2}$ and is not sensitive to the trap anisotropy λ and (2) the minimum value of (ω_ℓ/ℓ) is however sensitive to the trap anisotropy and varies from 0.53 for $\lambda = 0.0058$ to 0.33 for $\lambda = 10$ for $N = 3 \times 10^5$ atoms and for a geometric mean frequency of 7.8 Hz. These values are considerably larger than $\Omega_{c,th}$ calculated from eq. (7.1).

The observed critical angular velocity is closer to the value given by eq. (7.4) than that given by eq. (7.1).

When a trap is rotated with small angular velocity with the condensate in it, the condensate is deformed in shape; however it does not rotate with the trap [24]. Madison *et al* [25] created a rotating trap by shining two focussed spots of far-detuned laser beams travelling parallel to the axis of the trap and rotated the two beams about the axis. The anisotropy parameter ϵ was switched on slowly not to excite any surface mode frequencies. The parameter, $\bar{\Omega} = \Omega/\omega_\perp$ was varied slowly to a final value between 0.5 to 1.5 keeping ϵ fixed at 0.025 in the first study. In the

second study $\bar{\Omega}$ was kept fixed between 0.71 and 0.77 and ϵ was slowly increased to a final value in the range from 0 to 0.032. These experiments support the idea that vortex nucleation takes place when the surface barrier vanishes. However, the critical value of $\bar{\Omega}_{\rm c}$ was found to be between 0.71 and 0.77. This value of the critical frequency is considerably higher than the value 0.53 calculated by Dalfovo *et al* [23].

This discrepancy is sought to be explained in two different ways. The first explanation is as follows. By the use of a two-point laser beam to rotate the trap, one is preferentially generating the quadrupolar surface mode $\ell = 2$. The instability of this surface mode will occur at a rotation frequency $\bar{\Omega} = 0.7071$ which is close to the observed value. This implies that if we use a three- or four-point rotation of the trap with a laser we might excite preferentially the $\ell = 3$ or 4 surface mode. Then the value of $\bar{\Omega}$ at which vortex creation takes place will correspond to the instabilities of the corresponding surface modes. In other words, there should be a resonant excitation of vortices at different frequencies depending on two-, three- or four-point rotation of the trap.

A different explanation has been offered by Feder *et al* [26]. According to these authors a condensate with a vortex first becomes stable at a metastable frequency $\Omega_{\rm m}$. At this frequency, *any* infinitesimal displacement of the vortex from the axis increases the energy per particle. Below this frequency the vortex is unstable to any deformations. One may also state this in the following way. The Bogulibov excitation spectrum should only consist of excitations with a positive energy. Bogulibov excitations with negative energy $\epsilon_{\rm a}$ are called 'anomalous' modes. In a rotating condensate these anomalous modes are Doppler-shifted upwards by the rotation. The metastability rotation frequency $\Omega_{\rm m} = \max|\epsilon_{\rm a}|/\hbar$. These anomalous modes describe the precession of the vortex core about the origin of the trap. If $\Omega > \Omega_{\rm m}$, the precession is in the same direction as the motion of the superfluid around the core.

In an oblate trap with a disc-shaped condensate there is only one anomalous mode giving rise to a metastability frequency $\Omega_{\rm m} = 3/5\Omega_{\rm c}$. In such a case the critical rotation frequency coincides with $\Omega_{\rm c}$, the frequency at which surface barrier becomes zero. But for prolate traps in which the condensate is cigar-shaped there are many anomalous modes, the number increases as the ratio $\lambda = \omega_z/\omega_\perp$ decreases. It can happen that the metastability frequency can be considerably higher than $\Omega_{\rm c}$.

Experiments were performed with two-, three- and four-point rotation of the trap using two, three or four focussed laser beams travelling parallel to the axis of rotation [27]. The waist of the focussed beam could be changed from 5 μm to 25 μm. The condensate of 5×10^7 atoms of sodium, cooled well below $T_{\rm c}$, had a Thomas–Fermi radius of 27 to 30 μm perpendicular to the axis of rotation. With a two-point rotation, the laser beam of waist 25 μm was rotated with a radius of 25 μm around the z-axis. With three- and four-point rotations with the same beam waist, the radius of the circle of rotation was 55 μm. The large waist of the focussed laser beam corresponds to stirring the condensate with a wide spoon. After stirring for 500 ms, the laser beams were instantly shut off and the condensate was equilibrated once again for 500 ms. Then the cloud was allowed to expand ballistically for 41 ms before it was absorption imaged. The number of vortices in the condensate is plotted as a function of stirring frequency for two-, three- and four-point imaging. The results are shown in figure 7.

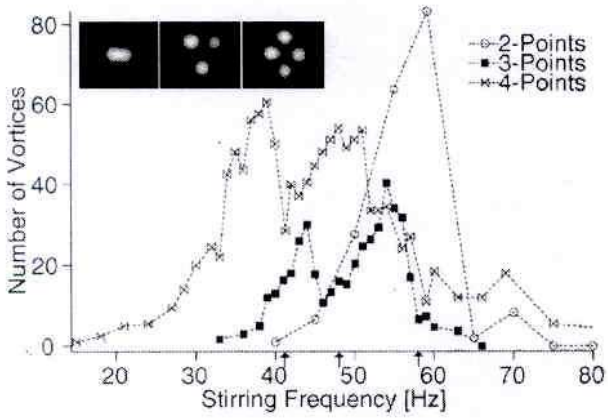

Figure 7. Number of vortices in the condensate as a function of frequency for two- (○) three- (●) and four- (×) stirring with a laser beam of waist 25 μm [27]. Arrows indicate the values of ω_ℓ/ℓ for $\ell = 2$, 3 and 4.

From the figure, it is seen that there is a maximum in the number of vortices produced when the rotation frequency, $\Omega = \omega_\ell/\ell$. The resonant excitation of the vortices supports the contention of a surface mode instability giving rise to the vortex state.

Experiments were also performed with a two-point rotation with a laser beam of waist 5 μm. This corresponds to stirring the condensate with a small spoon. In this case there was no resonant creation of vortices. Vortices were continuously created in increasing numbers as the speed of rotation was increased. The critical angular frequency $\bar{\Omega}$ was found to be 0.25 in agreement with the thermodynamic critical frequency. The radius of the circle in which the laser beam was rotated was varied. It was found that for a given angular frequency of rotation maximum number of vortices were created not when the laser beam was rotated at the edge of the cloud, but when it was rotated well inside the cloud. This implies that surface instability is not playing a role in the creation of vortices in this case. A different mechanism for vortex nucleation is responsible.

The conclusion is that while instability towards surface excitations is certainly one of the mechanisms for nucleation of the vortex, there could be other mechanisms involved.

8. Precession of a vortex

A vortex may be formed not at the centre of the condensate but slightly away from the centre. In such a case the vortex is subjected to a lateral force arising from the density gradient in the condensate. This lateral force gives rise to a Magnus effect i.e. the vortex is displaced in a direction perpendicular both to its axis and the transverse force arising from the density gradient. The vortex then precesses about the z-axis. In addition the vortex may experience a damping force. In such a case the precession is in a spiral, the vortex moving away from the centre to the edge.

Such a precession was seen [28] in a two-component condensate of ^{87}Rb in which a dynamical phase imprinting technique described earlier causes a vortex state in the ground state $|1\rangle$. The core of the vortex is filled with the atoms in the second component of state $|2\rangle$. This causes an enlargement of the vortex core and makes it possible to image the vortex core *in situ* by phase contrast imaging. A sequence of pictures at intervals of a few milliseconds show the precession of the vortex.

9. The vortex lattice

In the early experiments described in [11] only a small number of vortices were formed. However, the first experiments to create a very large number of vortices were conducted by Abo-shaeer *et al* [14]. The conditions of the experiment have been described in §5.3. As many as 130 vortices were created.

Tkachenko [29] quoted in ref. [14] has shown that the vortices arrange themselves in a perfect triangular lattice when a large number of vortices are created in an infinitely large condensate. However, in a finite condensate theoretical calculations [29,30] predicted circular distortions near the boundary.

In the experiments of Abo-shaeer *et al* [14] a thin slice of 50 to 100 μm in the centre of the cigar-shaped condensate containing vortices was optically pumped to the state $F = 2$, and was imaged after ballistic expansion which increased the core size by a factor of 40. The ballistic expansion was initiated after different hold times of the condensate in the trap after rotation of the trap was stopped. Figures 8A–H taken after different hold times indicates the growth of the vortex lattice and its subsequent decay.

From the figure we see that first the vortices form an irregular array (figure 8A) but slowly adjust themselves (figure 8B) to form a perfect triangular lattice (figure

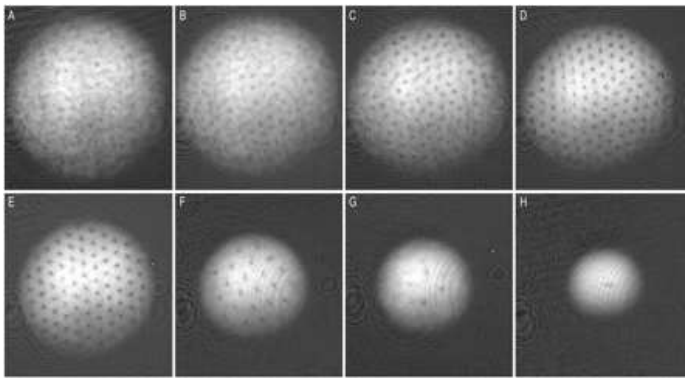

Figure 8. Growth and decay of the vortex lattice when a condensate of ^{23}Na was rotated in an axially symmetric trap and held in the trap for different times after the rotating laser beams were switched off. (**A**) 25 ms; (**B**) 100 ms; (**C**) 200 ms; (**D**) 500 ms; (**E**) 1 s; (**F**) 5 s; (**G**) 10 s and (**H**) 40 s. The temperature was below the condensation temperature such that 90% of the atoms were in the condensate. From ref. [14].

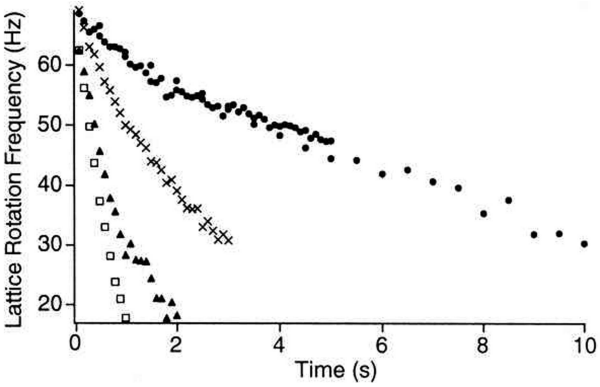

Figure 9. The decay of the number of vortices as a function of hold time in the trap for different amounts of condensate fraction from (31). Condensate fraction 0.78 (•); 0.75 (×); 0.71 (▲); 0.62 (□). From ref. [32].

8C) after 200 ms. Even at the edge of the condensate the lattice is perfectly regular unlike the theoretical expectations. The vortex lattice had a lifetime of several seconds (figures 8E–G). Theoretical calculations indicate a lifetime of about 100 ms. The lifetime should be inversely proportional to the number of vortices.

Occasionally one could see dislocation line and grain boundaries in such a vortex lattice.

Abo-shaeer *et al* [32] made further studies on the decay and growth of the vortex lattice as a function of temperature. They measured the number of vortices left in the condensate as a function of hold time in the trap after the condensate had equilibrated after switching off the rotating laser beams. The temperature of the condensate was varied to increase the fraction of atoms in the thermal state. Figure 9 shows the decay of the number of vortices in the condensate as a function of hold time in the trap for different condensate fractions. From this figure it appears that the decay is exponential. The characteristic decay time changes by a factor of seventeen as the condensate fraction is decreased from 0.78 to 0.62.

When the trap is rotated at high speed both the condensate and the thermal fractions rotate together. This was verified by non-destructive imaging of the rotating condensate and the thermal cloud and calculating the speed of rotation from the aspect ratios of the condensate and the thermal cloud. The results indicate that the thermal cloud is also co-rotating with the condensate.

The decay of energy of the vortex lattice takes place in two steps, first by friction from the vortex lattice to the rotating thermal component and then by friction from the rotating thermal component to the trap anisotropy. The friction between the condensate and the thermal component is much larger than the friction between the thermal fraction and the trap anisotropy. This is shown by the fact that the thermal component rotates at nearly two-third the speed of the condensate. The calculation of the viscous relaxation time between the thermal cloud and the trap for a classical Boltzman gas [33] yields a value of about $5\tau_{\rm elas}$ where $\tau_{\rm elas}$ is the elastic collision rate. This gives a temperature dependence of T^{-2} for the relaxation time for a thermal cloud. The presence of the condensate increases the moment of inertia

of the cloud by a factor f, which has a temperature dependence of T^{-4}. Taking this factor into account the relaxation time for the vortex lattice should scale as T^{-6}. The decrease in vortex lifetime by a factor of seventeen as the condensate fraction decreases from 0.78 to 0.62 is roughly in agreement with this estimate. The magnitude of the relaxation rates (of the order of $1s^{-1}$) is also in agreement with the measured values.

On the other hand, the growth of the vortex lattice after stirring is stopped does not appear to depend sensitively on temperature. This result is surprising. Feder [34] has solved numerically the Gross–Pitaevski equation for a stirred condensate. The calculation indicates an irregular growth of vortices in the absence of dissipation. Addition of a dissipation term by hand causes the growth of the ordered vortex lattice. The origin of the dissipation was not identified. The present results suggest that the thermal cloud has no role to play in the growth. Further study is necessary to elucidate the growth of the vortex lattice.

10. Non-equilibrium effects due to anisotropic compression of the vortex lattice

Engels *et al* [35] produced a condensate rotating at an angular velocity of $0.95\omega_\perp$ containing about 130 vortices. These form a regular triangular lattice. The vortex lattice is rotating with the condensate. If a surface mode, $\ell = 2$, $m_\ell = -2$ is induced then the resultant distortion of the condensate rotates at 8.4 Hz relative to the vortex lattice while the surface mode $\ell = 2$, $m = +2$ rotates only at 0.4 Hz relative to the vortex lattice. So, as the elliptically deformed condensate rotates relative to the vortex lattice, an anisotropic compression of the lattice takes place at a fast rate in the first case and at a slow rate in the second case. Figure 10 shows what happens in the two cases.

When the large amplitude quadrupolar surface mode $m_\ell = -2$ is excited it produces an elliptical deformation of the condensate which increases in the plane perpendicular to the rotation axis from 0 to 40% in 300 ms. In the frame in which the vortex lattice is at rest the elliptic deformation rotates at 8.4 Hz. When the minor axis of the deformation becomes parallel to one of the lattice axis, the vortex cores are squeezed together till they overlap producing planes along which the density of atoms is very low. This is shown in figure 10b. A scan through the planes in the direction of the major axis shows a very large contrast. On the other hand, when the quadrupolar mode $m_\ell = +2$ is excited the elliptical deformation increases from 0 to 50% in about 250 ms. But with respect to the vortex lattice the deformation is only rotating at a slow frequency of 0.4 Hz. Here the long-range order of the vortex lattice is slowly lost as shown in figure 10c.

11. Tkachenko oscillations in rapidly rotating BEC

Tkachenko proposed that the vortex lattice in a superfluid should support transverse shear waves. These waves have been observed by Coddington *et al* [36] in a rotating condensate of ^{87}Rb. A condensate containing about 2×10^6 atoms was set in rotation at an angular frequency Ω ranging from 0.84 to $0.975\omega_\perp$ ($\omega_\perp$ is the

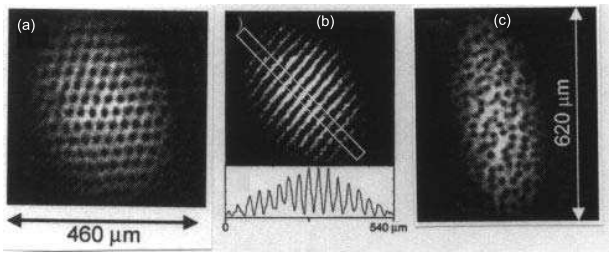

Figure 10. Rotating condensate (**a**) with a perfect vortex lattice arrangement when no quadrupolar surface mode is excited; (**b**) sheet-like structures due to merging of vortex cores along the minor axis of the condensate when the quadrupolar surface mode $\ell = 2$, $m_\ell = -2$ is excited and; (**c**) irregular distribution of vortices when the surface mode $\ell = 2$, $m_\ell = +2$ is excited. From ref. [34].

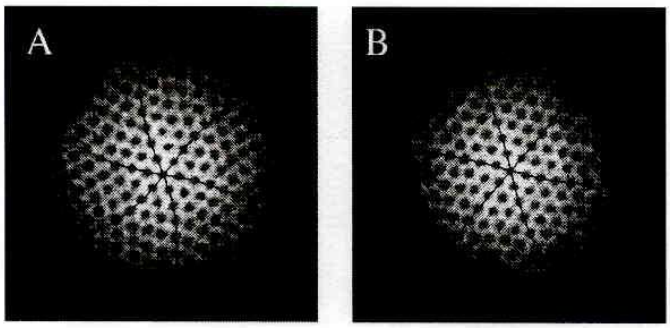

Figure 11. (1,0) Tkachenko mode excited by atom removal (**A**) taken 500 ms after the end of the blasting pulse, (**B**) taken 1650 ms after the end of the blasting pulse. BEC rotation is counterclockwise. Lines are sine fits to the vortex lattice. From ref. [36].

radial trap frequency $2\pi \times 8.3$ Hz). To create a shearing force on the vortex lattice the following techniques were adapted. In the first technique, a focussed resonant laser beam was sent along the axis of the condensate. Atoms are blasted out of the condensate due to the recoil velocity from a spontaneously scattered photon. Then the angular momentum per particle increases and causes an expansion of the radius of the cloud. This implies a radial outward flow of the fluid near the edge of the condensate. On the other hand, the fluid near the centre flows inwards to fill the void created by the blasted atoms. The Coriolis force due to rotation bends the outward and inward flows of the fluids in the opposite directions perpendicular to the direction of flow. This causes the vortex lattice to be sheared. In the second method, a red detuned laser beam is focussed near the centre of the condensate. This increases the density at the centre by the inward flow of the fluid. The deformation of the vortex lattice is imaged at different times after the blasting operation. Figure 11 shows the (1,0) Tkachenko mode of the vortex lattice.

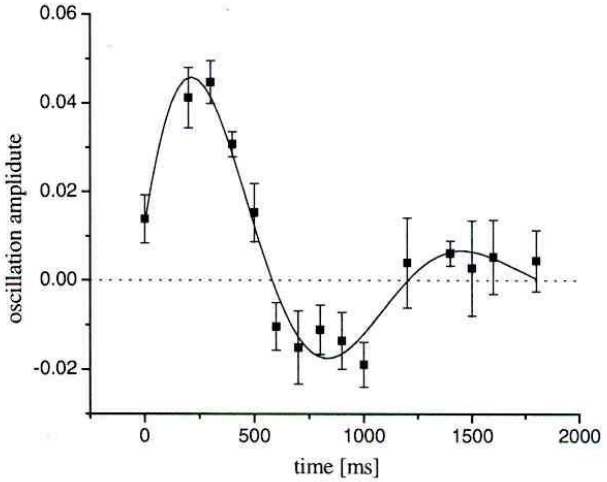

Figure 12. Variation of the amplitude of the s wave as a function of time. From ref. [36]

Anglin [37] calculated the frequency of Tkachenko modes in the xy plane, assuming the vortices to extend to infinity along their length (i.e. in the 2D approximation). The modes are characterised by two integers n and m, n denoting the radial nodes and m the the angular nodes. The S-shaped displacement of the lattice points can be fitted to a sine wave. The frequency is measured by the time variation of the amplitude of the S bend as shown in figure 12. The period of oscillation is however smaller than the theoretical value of Anglin, namely

$$\nu_{1,0} = 1.43\epsilon\Omega/2\pi.$$

The observed value is only 0.70 of the predicted value at the lower rotation rates. The disagreement becomes larger at larger rotational speeds. This disagreement has been theoretically resolved [38].

The authors have also observed the (2,0) Tkachenko mode.

12. Rapidly rotating Bose condensates: Softening of the Tkachenko mode

When the angular rotation frequency approaches $\omega_\perp$, the system becomes analogous to electrons in a strong magnetic field. In particular, the single particle energy states organize themselves into Landau levels like a two-dimensional electron gas in a strong magnetic field. In such rapidly rotating condensates, quantum Hall-like properties should emerge [39]. If the interaction energy is less than the cyclotron energy, $\hbar\Omega$, the lowest Landau levels are occupied. Depending on the filling factor N/N_v, where N is the number of atoms and N_v the number of vortices, different regimes of behaviour can be identified. When the filling factor is high, the system is in the mean field quantum Hall-like regime [40,41] and forms an ordered vortex lattice. As the filling factor decreases the shear strength of the vortex, lattice drops

leading to Tkachenko oscillations of reduced frequencies. For filling factors less than 10, a vortex lattice melting is predicted [39,42]. For still smaller filling factors one should observe quasi-particle excitations with fractional statistics.

Schweikhard *et al* [43] have verified that the frequency of the Tkachenko oscillations decreases in a rapidly rotating condensate of ^{87}Rb when the condensate atoms are removed. They start with a condensate of rubidium atoms spinning at an angular frequency of $0.95\omega_\perp$. The angular frequency is increased by illuminating the condensate uniformly by resonant laser light. The recoil velocity from spontaneous emission blasts atoms out of the condensate irrespective of their position. Because of the loss of atoms the cloud radius decreases and the cloud speeds up to keep the angular momentum per particle constant. Starting with 5×10^6 atoms the blasting operation is carried out for two seconds to reduce the number of atoms in the trap to 5×10^4. At this number the angular frequency of rotation of the condensate is $0.99\omega_\perp$. At this speed the cloud is highly oblate (disc-shaped) and one enters the quasi-2D regime.

The Tkachenko modes were excited by shining a red detuned laser beam along the axis of the condensate. Figure 13 shows the Tkachenko mode excited for $N = 1.5 \times 10^5$ atoms and at a rotational frequency of $0.978\omega_\perp$. Figures 13a and b show the displacements of the vortex lattice at $t = 0$ and $t = 1$ s.

We define a parameter $\Gamma_{LLL} = \mu/(\hbar\Omega)$. Since $\bar{\Omega}$ is only varied between 0.94 to 1, the change in Γ_{LLL} arises from the change in chemical potential μ which depends on the total number of particles. When Γ_{LLL} is more than 5 and for $\bar{\Omega}$ up to 0.96, the experimental results are in agreement with the predictions in the Thomas–Fermi approximation. The interaction energy is large compared to the cyclotron energy $\hbar\Omega$.

However, when Γ_{LLL} is reduced from 5 to 2, and $\bar{\Omega}$ is increased beyond 0.96, the frequency of the Tkachenko mode falls below the theoretically calculated values in the T–F approximation and approaches the theoretical values for the quantum-Hall state. This indicates a softening of the shear elastic constant of the vortex lattice. However it was not possible to track the Tkachenko modes below a Γ_{LLL} of 2.

There is a second prediction as a consequence of a change in the value of Γ_{LLL}. This concerns the fractional core area of the vortices, defined by $A = n_\mathrm{v}\pi r_\mathrm{c}^2$ (n_v is the areal density of vortices and r_c the core radius) as Γ_{LLL} is reduced. The experimental result of the variation of fractional core area of vortices with $(\Gamma_{LLL})^{-1}$ is shown in figure 14.

It is seen that, as one increases $(\Gamma_{LLL})^{-1}$ the fractional core area increases and saturates in the quantum-Hall regime. A simple-minded approach indicates that the vortex cores should merge i.e. A should tend to unity as $(\Gamma_{LLL})^{-1}$ increases. This is not in agreement with the experimental result. But according to the treatment of Baym and Pethick [44], A should saturate at a value of 0.225. This is roughly in agreement with the experiment.

13. Giant vortices

A giant vortex region is defined as a region of multiple vorticity with a depletion of density of the condensate. It may refer to a single vortex region with vorticity

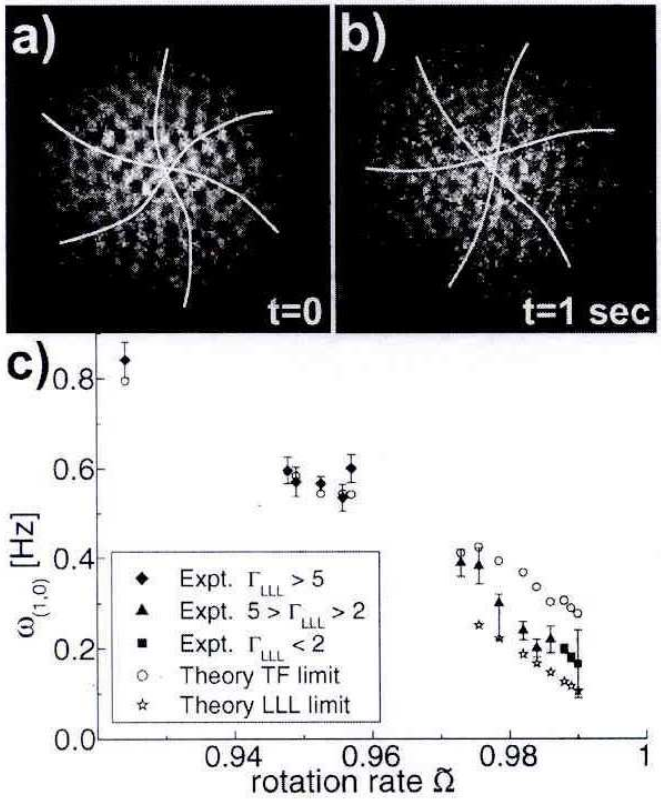

Figure 13. (**a**) and (**b**) show the Tkachenko mode at $t = 0$ and at $t = 1$ s for a condensate of 1.5×10^5 atoms and $\bar{\Omega} = 0.989$. The mode has not even completed a quarter of its period of oscillation. (**c**) Comparison of Tkachenko mode frequency $\omega_{1,0}$ (solid symbols) with theoretical predictions on the Thomas–Fermi limit (circles) and the quantum-Hall regime (stars). From ref. [43].

$\kappa > 1$ or to a region in which there are many singly-quantised vortices which are so densely packed that they cannot be resolved. Such regions of multiple vorticity are predicted where there is a pinning potential for vortices [45]. However, in the condensates of alkali atoms one does not expect such centres.

The imprint of topological phase in a condensate by reversing the axial magnetic field will produce vortices with an even value of κ. Vortices with $\kappa = 2$ were generated in a condensate of sodium by this method [10].

Engels *et al* [46] generated such giant vortices in ^{87}Rb at rotation rates, $\bar{\Omega} = 0.95$. The rotation rate was determined from the aspect ratio of the condensate. The temperature was sufficiently below T_c so that no significant thermal fraction was present. The condensate was disc-shaped and the vortex lines were perpendicular to the disc. There were 180 vortices in the condensate with a radial extension $R_\perp$ of 66 μm. To increase the angular momentum per particle some of the atoms

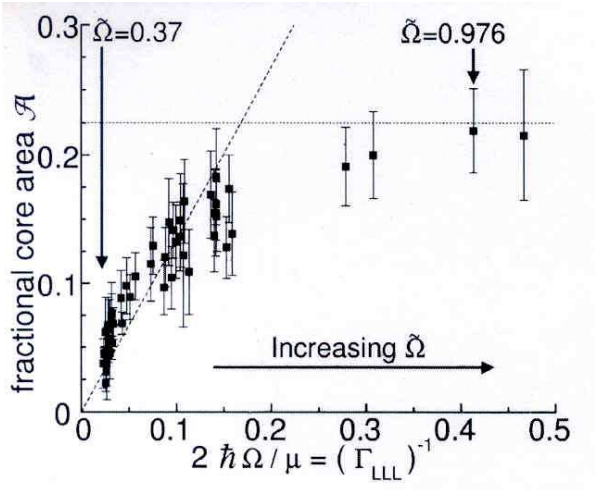

Figure 14. Fractional core area as a function of $(\Gamma_{LLL})^{-1}$. From ref. [43].

were blasted out by shining a focussed resonant laser beam of width 16 μm near the centre. With the increase in angular momentum per particle the number of vortices in the BEC is increased to more than 250.

A giant vortex appears if the atoms are removed strongly. The steps leading to the formation of the giant vortex are shown in figure 15.

As atom removal continues for 15 and 20 s, the lattice becomes disordered as shown in figures 15c and d. In figure 15e one sees the beginning of consolidation of the vortices in the core region. In figure 15f the giant vortex has grown. A close-up of the core region is shown in figure 15i. One sees the vortex cores in the centre merging with one another. The giant vortex develops further and becomes elliptical as seen in figure 15g and h. This elliptical deformation is the result of quadrupolar surface mode generated when the rotation frequency approaches the radial trapping frequency. The mode is generated by a slight ellipticity of the trapping potential.

On the other hand, if we apply the atom removal laser in a pulse then one obtains the sequence of figures as shown in figure 16.

When the atom-blasting laser of higher power (60 fW) is applied in a pulse of 2.5 s duration, a giant vortex appears as in figure 16b. If we keep the rotating condensate in the trap for 10 s after the atom-blasting laser is switched off then one gets figure 16c. Here we see that the giant vortex has broken up into singly-quantised vortices. In figure 16d taken after a hold time of 20 s, these singly-quantised vortices form a perfect lattice.

A stable giant vortex may also arise in a trap due to the quartic anharmonicity of the trap potential [47]. But in the trap produced in this experiment the ratio of the quartic term in the trap potential to the quadratic term was only 10^{-3} and the sign was opposite to the one expected to stabilize the giant vortex. So the authors do not believe quartic anharmonicity to be responsible for the stability of the giant vortex.

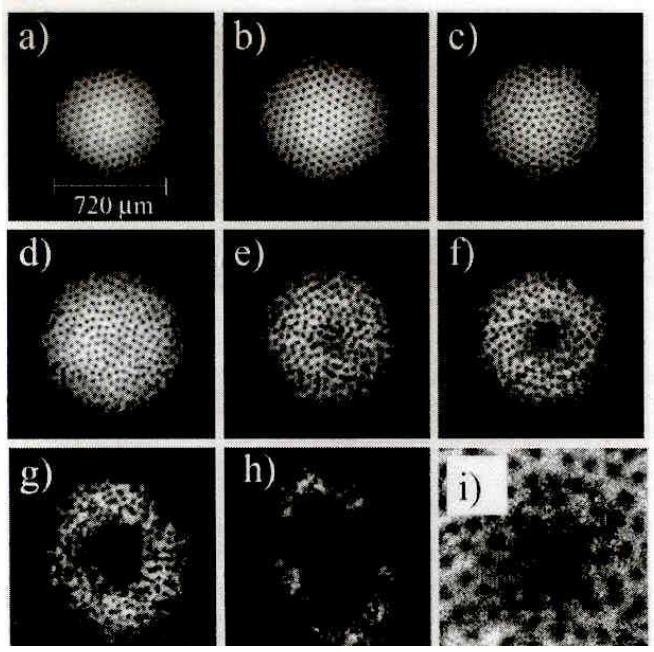

Figure 15. Stages in the formation of a giant vortex. Starting point is (**a**) with a condensate of ^{87}Rb with 180 vortices. Atoms are removed from near the axis by shining a 8 fW power for (**b**) 14 s. We now have 250 vortices due to decrease in the number of atoms. (**c**) 15 s, (**d**) 20 s, (**e**) 22 s, (**f**) 23 s, (**g**) = 40 s and (**h**) 70 s when light is on. (**i**) is a close-up picture of the core region in (f). From ref. [46].

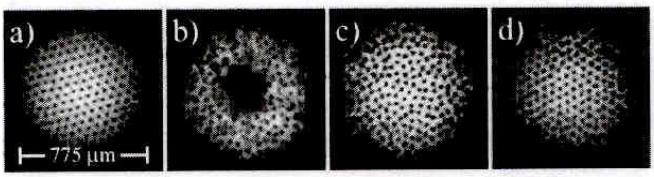

Figure 16. Lattice reforming after giant vortex formation. (**a**) The starting vortex lattice, (**b**) after a pulse of 60 fW for 2.5 s of the atom blasting laser. The hold time in the trap after the pulse is (**c**) 10 s and (**d**) 20 s.

The authors speculate that the giant vortex is produced by the Coriolis force. Because, as the atoms are removed from the centre, atoms from outside rush to fill the region, driven by the pressure gradient arising from the non-uniform density. The Coriolis force due to rotation sweeps these atoms around the centre giving rise to the large angular momentum.

14. Concluding remarks

A large amount of experimental work has come out in the last five years on vortices in rotating BEC. Many exciting results have been reported. A complete understanding of these results have not been gained.

I believe future experiments will concentrate on rapidly rotating condensates with a progressive reduction in the number of particles to probe the transition from the Thomas–Fermi to the quantum-Hall and to the fractional quantum-Hall regimes. The formation, stability and decay of giant vortices need to be probed further. In a spinor condensate the order parameter will not be a scalar. A paper has appeared on vortices in such condensates and this will also be an interesting field of research in future.

References

[1] M H Anderson, J R Ensher, M R Mathews, C E Wiemann and E A Cornell, *Science* **269**, 198 (1995)
[2] K B Davis, M O Mewes, M R Andrews, N J van Druten, D S Durfee, D M Kurn and W Ketterle, *Phys. Rev. Lett.* **75**, 3969 (1995)
[3] C C Bradley, C A Sackett, J J Tollett and R G Hulet, *Phys. Rev. Lett.* **75**, 1687 (1995)
[4] Franco Dalfovo, Stefano Georgini, Lev P Pitaevski and Sandro Stringari, *Rev. Mod. Phys.* **71**, 463 (1999)
[5] E Lundh, C J Pethick and H Smith, *Phys. Rev.* **A55**, 2126 (1997)
[6] J E Williams and M J Holland, *Nature (London)* **401**, 568 (1999)
[7] M R Mathews, B P Anderson, P C Haljan, D S Hall, C E Wieman and E A Cornell, *Phys. Rev. Lett.* **83**, 2498 (1999)
[8] B P Anderson, P C Haljan, C A Regal, D L Feder, L A Collins, C W Clark and E A Cornell, *Phys. Rev. Lett.* **86**, 2926 (2001)
[9] Mikko Mittonen, Naoki Matsumoto, Mikio Nakahara and Tetsuo Ohmi, *J Phys. Condensed Matter* **14**, 13481 (2002)
[10] A E Leanhardt, A Gorlitz, A P Chikkathur, D Kielpinski, Y Shin, D E Pritchard and W Ketterle, *Phys. Rev. Lett.* **89**, 190403 (2002)
[11] K W Madison, F Chevy, W Wohlleben and J Dalibard, *Phys. Rev. Lett.* **84**, 806 (2000)
[12] E Hodby, G Hechenblaikner, S A Hopkins, O M Marago and C J Foot, *Phys. Rev. Lett.* **88**, 010405 (2002)
[13] P C Haljan, I Coddington, P Engels and E A Cornell, *Phys. Rev. Lett.* **87**, 210403 (2001)
[14] J R Abo-shaeer, C Raman, J M Vogels and W Ketterle, *Science* **292**, 476 (2001)
[15] F Zambelli and F Stringari, *Phys. Rev. Lett.* **81**, 1754 (1998)
[16] P C Haljan, B P Anderson, I Coddington and E A Cornell, *Phys. Rev. Lett.* **86**, 2922 (2001)
[17] K W Madison, F Chevy, V Bretin and J Dalibard, *Phys. Rev. Lett.* **86**, 4443 (2001)
[18] B P Anderson, P C Haljan, C E Wieman and E A Cornell, *Phys. Rev. Lett.* **85**, 2857 (2000)
[19] Franco Dalfovo and Michele Modugno, *Phys. Rev.* **A61**, 23605 (2000)

[20] P Engels, I Coddington, P C Haljan and E A Cornell, *Phys. Rev. Lett.* **89**, 100403 (2000)
[21] K W Madison, F Chevy, W Wohlleben and J Dalibard, *J. Mod. Opt.* **47**, 2715 (2000)
[22] F Chevy, K W Madison and J Dalibard, *Phys. Rev. Lett.* **85**, 2223 (2000)
[23] F Dalfovo and S Stringari, *Phys. Rev.* **63**, 011601(R) (2000)
[24] A Recati, F Zambelli and S Stringari, *Phys. Rev. Lett.* **86**, 377 (2001)
[25] K W Madison, F Chevy, V Bretin and J Dalibard, *Phys. Rev. Lett.* **86**, 4443 (2001)
[26] D L Feder, A A Svidzinsky, A L Fetter and C W Clark, *Phys. Rev. Lett.* **86**, 564 (2001)
[27] C Raman, J R Abo-shaeer, J M Vogels, K Xu and W Ketterle, *Phys. Rev. Lett.* **87**, 210402 (2001)
[28] B P Anderson, P C Haljan, C E Wieman and E A Cornell, *Phys. Rev. Lett.* **85**, 2857 (2000)
[29] Tkachenko, quoted in ref. [14]
[30] Y Castin and R Dum, *Europhys. J.* **D7**, 399 (1999)
[31] L J Campbell and R M Ziff, *Phys. Rev.* **B20**, 1886 (1979)
[32] J R Abo-shaeer, C Raman and W Ketterle, *Phys. Rev. Lett.* **88**, 070409 (2002)
[33] D Guery-odelin, *Phys. Rev.* **A62**, 033607 (2000)
[34] D L Feder, quoted in ref. [29]
[35] P Engels, I Coddington, P C Haljan and E A Cornell, *Phys. Rev. Lett.* **89**, 100403 (2002)
[36] I Coddington, P Engels, V Schwekhard and E A Cornell, *Phys. Rev. Lett.* **91**, 100402 (2002)
[37] James Anglin, quoted in ref. [33]
[38] G Baym, *Phys. Rev. Lett.* **91**, 110402 (2003)
[39] N R Cooper, N K Wilkin and J M F Gunn, *Phys. Rev. Lett.* **87**, 120405 (2001)
[40] T L Ho, *Phys. Rev. Lett.* **87**, 060403 (2001)
[41] U R Fischer and G Baym, *Phys. Rev. Lett.* **90**, 140402 (2003)
[42] J Sinova, C B Hanna and A H MacDonald, *Phys. Rev. Lett.* **89**, 030403 (2002); **90**, 120401 (2003)
[43] V I Schweikhard, I Coddington, P Engels, V P Mogendorff and E A Cornell, *Phys. Rev. Lett.* **92**, 040404 (2004)
[44] G Baym and C J Pethick, cond-mat/0308325
[45] T P Simula, S M M Virtanen and M M Salomaa, *Phys. Rev.* **A65**, 033614 (2002)
[46] P Engels, I Coddington, P C Haljan, V Schweikhard and E A Cornell, *Phys. Rev. Lett.* **90**, 170405 (2003)
[47] E Lundh, *Phys. Rev.* **A65**, 043604 (2002)